



This is a repository copy of *Cross-section slenderness limits for columns with plastic rotations*.

White Rose Research Online URL for this paper:
<http://eprints.whiterose.ac.uk/113194/>

Version: Accepted Version

Article:

King, C. M. and Davison, J. B. orcid.org/0000-0002-6191-7301 (2014) Cross-section slenderness limits for columns with plastic rotations. *Journal of Constructional Steel Research*, 95. pp. 162-171. ISSN 0143-974X

<https://doi.org/10.1016/j.jcsr.2013.11.019>

Reuse

This article is distributed under the terms of the Creative Commons Attribution-NonCommercial-NoDerivs (CC BY-NC-ND) licence. This licence only allows you to download this work and share it with others as long as you credit the authors, but you can't change the article in any way or use it commercially. More information and the full terms of the licence here: <https://creativecommons.org/licenses/>

Takedown

If you consider content in White Rose Research Online to be in breach of UK law, please notify us by emailing eprints@whiterose.ac.uk including the URL of the record and the reason for the withdrawal request.



eprints@whiterose.ac.uk
<https://eprints.whiterose.ac.uk/>

Cross-section slenderness limits for columns with plastic rotations

C.M. King^{ab} and J.B. Davison^c

^a *Steel Construction Institute, Silwood Park, Ascot, Berkshire, SL5 7QN, UK*

^b *Buckland & Taylor Ltd, 101-788 Harbourside Drive, North Vancouver, BC, Canada V7P 3R7*

^c *Department of Civil and Structural Engineering, University of Sheffield, Sheffield S1 3JD, UK*

Abstract

This paper reports on a study of local inelastic buckling in square hollow section columns with large plastic rotations. The study was conducted as part of the validation of a proposed design method for discontinuous columns in braced frames in which plastic rotations in the columns are used to limit the moments in the columns. The study included both testing of full-scale columns and a parametric study by finite element analysis. The results demonstrate that current codes permit cross section slenderness in plastic sections which are likely to lead to premature buckling in structures using plastic (inelastic) design if the rotations are large. Design limits are proposed for square hollow sections relating cross-section slenderness to column end rotations.

Keywords. Discontinuous column; tube wall slenderness; ductility requirements; rotation capacity; local buckling

1 Introduction

A new form of braced frame has recently appeared in Britain for residential construction in which the columns are discontinuous [1]. Rather than passing over a number of storeys, each column is only one storey high and is fitted with a base and cap plate to bolt to the beams below and above, as shown in Figure 1 [2]. Columns are square hollow sections with the smallest possible external size so they can be hidden in the thickness of the walls. The beams are continuous and pass over the top of the columns thus requiring little in fabrication yet benefitting from the efficiency of continuity. However, this continuity of the beams may cause some rotation to be induced at the top and bottom

of the column under certain loading arrangements resulting in curvature of the column, which would reduce the resistance of the column below that of a pin-ended strut.

The behaviour of discontinuous columns is significantly affected by two issues (i) the stiffness of the column-beam joint (ii) the effect of bending moments in the columns on the compression resistance. At the top of a building, the axial compression in the columns is small and if relatively thin column end-plates are used, the connections will be flexible so the beam can rotate relative to the columns. This would result in higher sagging moments in the beams than would be calculated in a rigid frame analysis. At the bottom of a building, the axial compression is high and this compression clamps the columns and beams so that very little rotation of the beam relative to the column is possible, so the frame resembles a continuous one. If the frame is analysed elastically as a continuous frame, the designer must either determine the stiffness of the joints (which means including the effect of axial compression) or specify end-plates so thick that the joint is sensibly rigid even for low axial compression. In a continuous frame, the bending moments in the columns calculated by elastic analysis can be of such a magnitude that they cause a significant reduction in the resistance to axial compression. To compensate for this, larger column areas are required, increasing the bending stiffness and attracting more bending moment. This may lead to heavy columns, negating one of the attractions of the construction method which is to have small column cross-sections to allow them to be hidden in walls or limit the visual impact of exposed columns.

The application of traditional design methods which might be used to design a frame with discontinuous columns is unsatisfactory for a number of reasons. For example, the use of the 'simple construction' method [3] (in which the beam is assumed to be supported by a cap plate) is compromised by the practical effects of using end plates of sufficient thickness to satisfy UK building regulations tying capacities. This necessitates the addition of a moment in the column arising from the column end rotation induced by the beam rotation (the stiffer the connection the

greater the column rotation) and the resulting calculated column capacities are relatively low. If joints are assumed to be rigid and elastic analysis is used, the column end moments will be large thus lowering the calculated column capacity and relatively expensive connection details will be required to be consistent with the analysis model. To analyse such frames rigorously taking into account joint flexibility requires considerable effort, making them economically unattractive to design offices. Other methods of design might include designing the frame plastically (provided it is braced independently) and allowing plastic hinges to develop in the columns [1,4] or allowing for the semi-rigid nature of the joint in an approximate manner. In reviewing available methods, early work by Gent and Milner provides an interesting approach, which is briefly outlined next.

1.1 Gent & Milner's column research

Gent published a paper in 1966 [5], followed by a second with Milner in 1968 [6], describing tests on small scale steel I-section columns subject to an initial end-rotation and then to increasing axial compression while the end-rotation remained applied. In the tests, end rotations were imposed at the two ends of the columns by moments applied through short cantilever beams loaded at their ends through a turnbuckle arrangement, as shown in Figure 2(a). Importantly, this system allowed the moment to *reduce* as the column ends rotated, just as the end moments of a fixed-ended beam reduce if the end restraints are allowed to rotate. Initially the column had no axial load applied. The axial load was then increased and the end moment resisted was measured. The experiments showed that as the axial load was increased, the yielding of the column allowed such large end rotations that the columns “shed” the moments, as shown in Figure 2(b).

As the axial compression was increased the end moments reduced to zero and then changed to acting in the opposite direction to some small amount before the member failed by flexural buckling in the plane orthogonal to the plane of the web of the column, even when the end rotations were applied in the plane of the web. It is important to note that the end moment was applied by the turnbuckle system - it was not applied as an eccentric load on the column; application as an

eccentric load does not allow the moment to reduce as the column ends rotate and this is the design case assumed in codified checks of resistance to combined axial compression and bending.

Gent and Milner's tests showed that at the Ultimate Limit State in braced frames with rigid beam-column connections plasticity in the column reduced column stiffness thus limiting the bending moment attracted to the columns and also permitting more severe curvature in the columns. When moments are applied to the columns by the beams, the reduced column stiffness allows increased rotation of the column ends, tending to shed the applied moments provided that the beams can resist the moments shed by the columns. Gent and Milner [6] observed "that even under biaxial bending restrained columns have a remarkable capacity to sustain high axial loads by shedding end moments". Gent [5] wrote that "By considering limiting cases in this way, the design of the beams and the columns could largely be divorced". Although the papers propose a possible approach to design, it is not developed into a complete method. Experimental work by Davison et al. [7,8] and Gibbons et al. [9,10] on full size semi-rigidly connected braced steel frames demonstrated this same phenomenon and formed the basis of a design method which assumed the columns to be pin ended and ignored the column moments because at the ultimate limit state the beneficial restraining effect of the attached beams outweighed the detrimental effect of the diminishing moments as the column buckles [11,12].

1.2 Design using plastic rotations (moment shedding)

A new design method for discontinuous columns in braced frames was proposed by King [13] using moment shedding so that the columns are designed for zero end-moment even if the connection of the columns to the beams are effectively rigid. The proposed method is for square hollow section columns, assuming that the full cross-section is effective. The columns are assumed to derive no stability from the adjacent beams and are assumed to be in single curvature because this results in

1 the lowest resistance to axial compression. The possible rigidity of the connection is used to
2 determine the end-rotation of the column which the column is designed to resist. The columns are
3 designed to resist the applied axial compression plus the coexistent moment at mid-height resulting
4 from the greatest end-rotation of the adjoining beam plus the additional moment arising from a
5 design imperfection. The design imperfection is calculated so that the resistance of the
6 discontinuous column cannot exceed the buckling resistance of a pin-ended strut. The design model
7 is equivalent to a rigid-plastic pin-ended column with a plastic hinge at mid-height and with an
8 offset from the line of thrust.
9

10
11
12
13
14
15
16
17
18
19
20 To verify the proposed design method, a series of tests was required both to demonstrate the
21 resistance to axial compression and to establish the requirements for slenderness of the cross-
22 section (c/t in Eurocode 3 or b/t in most other design codes). The slenderness requirements of
23 existing codes had been noted as a possible issue by King [13] following calculations using an
24 approximate closed solution to local inelastic buckling in the presence of high longitudinal plastic
25 strains.
26
27
28
29
30
31
32
33

34 **2.0 The test programme**

35
36
37 The test programme is shown in Table 1. All specimens were Celsius¹ 355 120×120 Square Hollow
38 Sections (SHS). As the purpose of the testing was to provide data for use in validating the proposed
39 design approach, it was desirable to have more than one test so that repeatability could be
40 investigated. The most common applications of discontinuous columns tend to require thick wall
41 columns to reduce the column section size to the minimum hence more tests were performed on
42 sections with 10mm wall thickness than with thinner walls. Testing at full scale allowed the effect
43 of slender walls to be investigated experimentally by using both a thick and a thin walled section of
44 the same serial size.
45
46
47
48
49
50
51
52
53
54
55
56

57
58 ¹ Celsius is the brand name for structural grade hot-finished hollow sections produced by Tata to EN 10210 in steel
59 grade S355J2H.
60
61
62
63
64
65

1 The yield stress of the test columns were measured from coupons cut from most of the specimens
2 after the tests were completed as shown in Table 2.
3
4
5

6 **2.1 Test rig and instrumentation**

7
8
9 Full-scale specimens were tested in a hydraulic two-post rig as shown in Figure 3. Although the rig
10 is normally operated under load control rather than displacement control, with skill the
11 displacement can be controlled by limiting the flow of oil from the pump to the jack. Using this
12 control technique, very smooth curves were recorded on the falling branch of the plot of load versus
13 displacement.
14
15
16
17
18
19
20
21
22

23
24 End-fittings or “shoes” were manufactured to fit to the ends of the specimen without fastening thus
25 avoiding fabrication work on the specimen themselves, so the plane SHS sections supplied could be
26 used directly. The shoe at the bottom of the test column is shown in Figure 4 and the shoe at the top
27 of the column was similar. Articulation about a cylindrical pin ensured that the deformation of the
28 column was in one predetermined plane. The use of these shoes introduced some friction, which
29 was evaluated through unload/re-load cycles, and added 75mm to each end of the column ie the
30 overall length of the strut was 2650mm from centre of roller to centre of roller. This length is
31 representative of domestic construction and the longest piece that could be fitted within the
32 available test-rig.
33
34
35
36
37
38
39
40
41
42
43
44
45
46
47

48 The shoes were adjusted to give an eccentricity of $L/750$ in the column to simulate the geometric
49 imperfections that might be experienced in practical construction. The initial imperfections were
50 measured and the maximum value recorded was $L/1600$.
51
52
53
54
55
56
57

58 The instrumentation on each specimen consisted of an in-plane and an out-of-plane inclinometer at
59 the top and bottom of the column and, at column mid-height, two LVDTs to measure in-plane
60
61
62
63
64
65

deflection (one on each side of the column) and a single LVDT to measure deflection out of plane.

The LVDTs were connected by wires to a spring-grip frame (shown in Figure 5) shaped to avoid displacements arising from local deformations of the walls by fitting the section at all four corners.

The inclinometers were attached directly to the specimen at 200mm from the centres of the pins.

Only in-plane rotations were measured in the pilot tests (kc1 and kc2) and tests kc8, 9 and 10. Axial shortening was measured by the ram movement so included the extension of the posts of the rig.

The ram displacement within the jack was measured by an externally mounted LVDT on the lower loading platten and the jack force was determined by a pressure transducer fitted to the hydraulic circuit of the machine.

2.2 Test results

The strain rate was as slow as reasonably practical with the test equipment used. However, it proved impossible to limit the unloading rate to be as slow as the loading rate. This is because, after maximum load, the distance between the end-bearings of the test-rig is decreasing but the overall length of the column is increasing as a result of the reduction in compressive strain. This increase in the overall length of the column together with the decrease in distance between the end-bearings causes an increase in the mid-height deflection which further reduces the compression resistance of the column. The growth of the mid-height deflection is a dynamic effect. Therefore some dynamic effects were expected in the results measured after maximum load. To give an indication of the scale of the dynamic effect, the duration of the tests is listed in Table 3.

The test results proved to be broadly as predicted with all the tests showing a long falling branch after maximum resistance. The general form of the results was very similar for all the tests except for the loss of strength due to local inelastic buckling in the thinnest wall sections at end rotations greater than 40 milliradians. Different aspects of the results are discussed below.

2.2.1. The unloading/re-loading cycle

The test curves confirm the shape of the falling branch as predicted by analysis. However, it was necessary to choose an arbitrary static point on the falling branch of the test curve to allow a precise comparison with the analyses which assumed static equilibrium. The static point was established by unloading the test. The test was then continued to complete the test curve to the desired end-rotations.

2.2.2. In-plane displacements

Plots of load versus mid-height displacement in the plane of buckling are shown in Figure 6.

The mid-height displacements differ between tests during the initial loading up to the maximum load. This is shown more clearly in the inset plot in Figure 6 which shows the displacements at a larger scale. This shows that the tests cover a wide range of imperfections as might be expected in practical construction.

2.2.3. Out-of-plane displacements

It was intended that the out-of-plane displacements should be limited to small values relative to the in-plane displacement by the design of the end fittings. The plots in Figure 7, which shows the out-of-plane displacement plotted against the in-plane displacement for each test, shows that this was achieved even when large in-plane displacements occurred along the falling load- displacement branch seen in Figure 6.

2.2.4. In-plane end rotations

Plots of axial load versus mean end-rotation (i.e. average of the top and bottom values) are shown in Figure 8. This shows that the load/end-rotation from all the tests have long falling branches as

1 expected. The figure also shows as horizontal lines the design values of resistance of the three
2 sections when calculated to EN 1993-1-1[14] as pin-ended struts.
3

4
5 The plots for the two tests on specimens with 5mm wall thickness (kc 6 and kc 10) show marked
6 reductions in resistance below the general trend due to local inelastic wall buckling, which was
7 expected. It is interesting to note that kc10 has a higher maximum resistance than kc6 but has a
8 lower rotation capacity before the dramatic loss of resistance at about 50 milliradians. This
9 suggests that the lower yield of kc6 produced a more uniform curvature which was lower than the
10 curvature of kc10.
11
12
13
14
15
16
17
18
19

20
21 Plots with the maximum load normalised are shown in Figure 9. These plots show how similar the
22 behaviour is up to the rotation at which local inelastic buckling of the wall precipitates a drastic loss
23 of resistance. It is difficult to identify the individual tests in Figure 9 but the important point is that
24 all the tests are similar except that the 5mm wall tests (kc6 and kc10) drop significantly from about
25 50 milliradians.
26
27
28
29
30
31
32
33

34 35 36 **2.3 Comparison of test data with the proposed design model**

37
38 The test results show that the moment shedding predicted by King [13] occurs in full-scale columns.
39 Figure 10 shows the results from tests of two columns with the thickest walls compared with graphs
40 derived from the simplified design method by King by calculating the design imperfection from the
41 maximum compression resisted in the test instead of the compression resistance calculated from a
42 design code.
43
44
45
46
47
48
49
50

51 **3.0 Effects of breadth to thickness ratios of wall**

52
53 It is well known that the stability of elements in compression depends upon the magnitude of the
54 compressive stress and the slenderness of the element. In design codes, the stability is verified by
55 calculating the breadth to thickness ratio (b/t) of the components of each cross-section and
56 comparing them with a limiting value. Currently, design codes rely on a single value of limiting
57
58
59
60
61
62
63
64
65

breadth to thickness ratio for cross sections allowed to sustain plastic rotations. However, in members allowed to sustain plastic rotations, the curvature may be severe when loaded. In these circumstances, the local stability is dominated by the out-of-plane force on the element caused by the axial compressive stresses and the curvature. Hence, a single limiting value cannot ensure the local stability of the cross-section for all rotations. For cross-sections sustaining plastic rotations, design codes should either give a limit to the curvature for which the single value of b/t for plastic behaviour is safe or they should give limiting values for different curvatures

The effect of breadth to thickness ratios of the walls of hollow sections was investigated by King [13] using a closed solution for local inelastic buckling including the effects of plastic flow caused by longitudinal strains exceeding yield strain. This investigation included a 140×140 square hollow section, 3 metres long, in single curvature with end rotations of 40 milliradians. This end rotation is possible at Ultimate Limit State (ULS) for beams with Permanent (Dead) Load that is about twice the Variable (Live) Load, using common deflection limits for the Serviceability Limit State and accounting for some plasticity in the beam at ULS.

The investigation demonstrated that b/t must be increased for increased curvature of the member if the walls are to remain stable. This cast doubt on the reliability of a single value of b/t for plastic design, as commonly used in modern design codes.

3.1 Slenderness limits in Codes of Practice

Requirements of Eurocode 3

For a hot-finished square hollow section designed to Eurocode 3 [14], the slenderness limits for sections is expressed as $c/t = 33\varepsilon$ for Class 1, where c is the width of the internal flat face and $\varepsilon = \sqrt{(235/\text{yield})}$. According to Annex A3 of EN 10210-2 [15], the internal corner radius may be taken as 1.0 times the wall thickness. For members with yield stress of 355 MPa, $\varepsilon = \sqrt{(235/355)} = 0.814$. Therefore, for the flat face, $c/t = 33 \times 0.814 = 26.9$ for Class 1.

Requirements of AISC 360-10

1 AISC 360-10 [16] has limits for b/t ratios in two sections. Chapter B, Design Requirements, Table
2 B4.1b, gives the compact/non-compact limit of $1.12\sqrt{(E/F_y)}$ for flanges of beams of rectangular
3 HSS and boxes of uniform thickness. For members with yield stress of 355 MPa, this gives the
4 limiting $b/t = 1.12\sqrt{(200,000/355)} = 26.6$, where b is the internal flat face. This is similar to the limit
5 given in EN 1993-1-1 for Class 1 members in general. For plastic design of columns, Appendix 1,
6 Design by Inelastic Analysis, section 1.2.2b, gives the limit of $0.94\sqrt{(E/F_y)}$ for flanges of
7 rectangular HSS and boxes of uniform thickness. For members with yield stress of 355 MPa, this
8 gives the limiting $b/t = 0.94\sqrt{(200,000/355)} = 22.3$, where b is the internal flat face.
9

10 **3.2 Test results**

11 The range of wall thicknesses of the test columns was chosen to study the effect of the breadth to
12 thickness ratio as noted in Table 1. Taking the predictions by King [13] for a 140×140 square
13 hollow section 3 metres long and multiplying the wall thickness by the ratio of the member
14 breadths, 120/140, the walls of the 120×120×6.3 SHS in tests kc5 and kc9 were expected to be
15 stable at end-rotations greater than 40 milliradians but the walls of the 120×120×5.0 SHS in tests
16 kc6 and kc10 were expected to be unstable at 40 milliradians.
17

18 The two columns with 5mm wall thickness, kc6 and kc10, show a clear drop in resistance to axial
19 load arising from local inelastic buckling from about 55 and 40 milliradians. This is seen in terms
20 of end-rotations in Figure 11. The two columns with 6.3mm wall thickness, kc5 and kc9, show only
21 a very slight reduction in axial resistance in the tests. The tests kc5 and kc9 show a small increase
22 in the downward slope of the axial load versus end-rotations curve from about 70 milliradians as
23 seen in Figure 11, indicating a reduction in resistance due to local inelastic buckling.
24

25 There was no drop of resistance due to local inelastic buckling for the 10mm wall columns, even at
26 the maximum test rotation.
27
28
29
30
31
32
33
34
35
36
37
38
39
40
41
42
43
44
45
46
47
48
49
50
51
52
53
54
55
56
57
58
59
60
61
62
63
64
65

The onset of local inelastic buckling with end rotation is shown for different b/t ratios in Table 4.

Here the wall slenderness is calculated as the internal flat width between internal radii (taken equal to the wall thickness) divided by the wall thickness, so, for a 120×120×5 SHS, $b/t = (120-4*5)/5 = 20$. The end rotations in the tests are large at the point of local inelastic buckling, but the columns were in single curvature. In real structures, columns are commonly in double curvature, so the magnitude of the curvature can be expected to be doubled. This reduces the stability of the wall for a given b/t ratio.

3.3 Parametric study for inelastic wall buckling

The design model proposed by King [13] assumes that the column is in single curvature to simplify the calculation of overall buckling resistance. However, many columns will be in double curvature, which results in higher curvatures than in a column in single curvature with the same magnitude of end rotation. Because the stability of the wall depends on the out of plane force on the wall (which is the product of the longitudinal force in the wall and the curvature of the wall) and plastic flow, the effect of higher curvatures needed investigation to find b/t ratios at which the walls of the section would be stable.

This effect was investigated by King [13] by a parametric study using finite element analysis. Finite element models were made and used to simulate the results of the tests on the 120×120 SHS sections. Abaqus was used to conduct geometric non-linear and material non-linear finite element analyses. The model (shown in Figure 12) used shell elements with the nodes and the mid-thickness of the elements in the plane of the centre-line of the walls of the column. This results in a model with square corners, which is slightly different from the tight radius corners of hot-formed SHS sections. The ends of the model are connected to a “spider” of rigid-body elements, whose legs radiate to the point of intersection of the centre-line of the column and the plane of the end of the column. Most analyses were conducted using a model of the entire column although the effect of mesh refinement was checked by using a half-model that comprised a column cut longitudinally

1 along the centre-line of two opposite sides [13]. The magnitude of the residual stress was not
2 measured due to financial constraints but was taken as 10% of the minimum specified yield stress of
3 the section, which is appropriate for hot-finished hollow sections, and followed a bi-triangular
4 pattern as illustrated in Figure 13. The analysis assumed elastic/perfectly-plastic non-linear material
5 behaviour.
6
7
8
9

10 The analyses were made using enforced shortening of pin-ended columns with the initial
11 imperfection in the plane of the end-rotations.
12

13 For the simulation of the tests on the 120×120 SHS sections, the yield stress from the test coupons
14 were used for each test. The only change to the geometry of the models was to adjust the
15 eccentricity of the application of load so that the end-rotations in the elastic range of the loading
16 cycle were the same as those measured on test. This ensured that the model had the same effective
17 eccentricity as the test specimen. The resulting curves from the finite element analysis were
18 generally close to the curves from the tests, especially in the range of higher end-rotations, which is
19 the region of interest for inelastic buckling of the walls. The only exception was test kc10 which is
20 discussed in more detail below.
21
22
23
24
25
26
27
28
29
30
31
32
33

34 For the parametric study of inelastic wall buckling, the same finite element model was used as for
35 the simulation of the tests on the 120×120 SHS sections because the performance had been shown
36 to be satisfactory by comparison with the full-scale tests. The same mesh was used, but scaled in
37 length and width to suit the desired length/breadth ratios. The size of sections modeled were
38 140×140 SHS sections because these had been identified as the largest sections used in the frames
39 recently constructed in the UK. Different thicknesses and different member lengths were used to
40 develop the greater curvatures experienced in members in double curvature. The effects with end-
41 rotations in a rectangular plane were investigated for columns in single curvature of lengths 750mm
42 and 1500mm to reproduce the behaviour of 140×140 SHS columns in double curvature of 1500mm
43 and 3000mm length. The results are shown in Figure 14; it can be seen that the wall stability is
44 more demanding for 750mm (the solid lines) than for 1500mm (the broken lines). For example, for
45
46
47
48
49
50
51
52
53
54
55
56
57
58
59
60
61
62
63
64
65

1 a 1500mm long member with wall thickness 6.3mm, the resistance starts to fall away from the
2 stable line (shown by the 12mm wall thickness section) at 20 milliradians end rotation whereas for a
3 750mm long member with 6.3mm wall thickness, the resistance starts to fall away from the stable
4 line (shown by the 10mm wall thickness member) at 30 milliradians end rotation.
5
6
7
8
9

10 Similar analyses were conducted for end-rotation in a plane at 45° to the rectangular planes as
11 shown in Figure 15. Comparison of Figures 14 and 15 shows that the local inelastic buckling
12 requirements for end-rotations at 45° are almost identical to those for end-rotations in a rectangular
13 plane. The breadth to thickness ratio above which local inelastic buckling impairs the column
14 resistance is shown in Figure 16 plotted against end rotation.
15
16
17
18
19
20
21
22
23

24 **3.4 Comparison of test results with Finite Element Analysis**

25
26

27 For studying the inelastic buckling of the wall, the most important part of the load-rotation curve is
28 the region of highest end rotations. In this region, the curves from the finite element analysis are
29 generally close to the curves from the tests. At the end of the test range, that is at the highest end
30 rotations, all the tests gave a slightly higher rotations for a given load except test kc10 which had a
31 5mm wall thickness. Figure 17 shows the two tests with 5mm wall thickness, kc6 and kc10. It can
32 be seen that test kc6 gave higher end-rotations at a given load than the finite element analysis, but
33 kc10 gave lower end-rotations at the point where there is a rapid fall in end rotation from 40
34 milliradians. This suggests that the finite element analysis model used may overestimate the end-
35 rotations at which the walls remain stable for the thinner walled sections. It is possible that the
36 difference was caused by variations in the wall thickness of the test specimen in contrast with the
37 uniform thickness assumed in the finite element model because specifications for hollow sections
38 allow more generous thickness tolerances than are commonly allowed for open sections.
39
40
41
42
43
44
45
46
47
48
49
50
51
52
53
54
55

56 The close correlation between the load-rotation curves for tests and analysis for the six tests with
57 wall thicknesses of 10mm and 6.3mm give confidence that the finite element model performs well
58
59
60
61
62
63
64
65

for the region of high end-rotations. The difference between the two tests with 5mm walls suggests that the inelastic buckling of lower wall thicknesses is more variable than for thicker walls.

3.5 Proposed design limits

The proposed design limits are defined by the curve “b/t from FEA” shown in Figure 16. These limits were derived for 140×140 square hollow sections of length 1500mm in double curvature i.e. a length/breadth ratio of 10.7. The limits for greater length/breadth ratios would be less onerous because for a longer member the change of angle between the ends is spread over a greater length thus reducing the severity of the curvature and lowering the out-of-plane forces on the cross-section walls. The numerical values are given in Table 5.

1
2
3
4
5
6
7
8
9
10
11
12
13
14
15
16
17
18
19
20
21
22
23
24
25
26
27
28
29
30
31
32
33
34
35
36
37
38
39
40
41
42
43
44
45
46
47
48
49
50
51
52
53
54
55
56
57
58
59
60
61
62
63
64
65

1
2
3 Given the difference between the finite element analysis and the test curves for test kc10, the
4
5 authors' recommend reducing the limiting end rotations shown in Table 5 by around 20% for b/t
6
7 values greater than 20; the revised values are shown in brackets in Table 5.
8
9

10 11 12 13 **4.0 Conclusions** 14

15
16 Tests have been performed on full-scale columns with different wall thicknesses, using
17
18 120×120 SHS sections, which were the largest that could be tested in the available test rig, with
19
20 the load applied to maximum resistance and then the hydraulic ram extension was continued to
21
22 measure the load versus end-rotation beyond maximum resistance of the column. The failure mode
23
24 was single curvature flexural buckling. Sections with 10mm wall thickness showed no local
25
26 inelastic buckling over the full range of the tests, whereas sections with thinner walls displayed
27
28 local inelastic buckling. Finite element analyses were made of the 120×120 SHS sections in the rig
29
30 using a non-linear geometry solution and elastic-plastic material properties. The curves of load
31
32 versus end-rotation from the finite element analysis are generally close to the curves measured in
33
34 the test rig.
35
36
37

38
39 A parametric study of inelastic buckling related to wall slenderness was then conducted using the
40
41 same finite element model scaled to investigate the rotation capacity of members with ratios of
42
43 length/breadth as low as 10.7 failing in double curvature. The study shows that the single values of
44
45 limiting b/t in modern codes are not sufficient to avoid local inelastic buckling when plastic (or
46
47 inelastic) analysis is used if the curvature of the members is high due to plasticity. The parametric
48
49 study was confined to square hollow sections, but the same issue of decreased stability with
50
51 increased local curvature will apply to all cross-sections.
52
53
54

55
56 With the increasing use of material non-linear behaviour of structural steel in industry, made
57
58 possible by the wider use of finite element analysis, design codes should either give a limit to the
59
60
61
62
63
64
65

curvature for which the single value of b/t for plastic behaviour is safe or they should give limiting values for different curvatures.

Acknowledgements

The authors wish to thank the Steel Construction Institute for funding the fees of the first author for the first two years of his PhD study and Corus (now Tata) for financial support of the experimental work.

1
2
3
4
5
6
7
8
9
10
11
12
13
14
15
16
17
18
19
20
21
22
23
24
25
26
27
28
29
30
31
32
33
34
35
36
37
38
39
40
41
42
43
44
45
46
47
48
49
50
51
52
53
54
55
56
57
58
59
60
61
62
63
64
65

References

- [1] British Constructional Steelwork Association/Steel Construction Institute. The use of discontinuous columns in simple construction. AD281 New Steel Construction, February; 2005
- [2] British Constructional Steelwork Association/Steel Construction Institute. Discontinuous columns in simple construction: Beam-column connections. AD288 New Steel Construction, July; 2005
- [3] British Constructional Steelwork Association/Steel Construction Institute. The use of discontinuous columns in simple construction. AD283 New Steel Construction, March; 2005
- [4] Wood RH. A new approach to column design. Building Research Establishment Report. Department of the Environment, HMSO; 1974.
- [5] Gent AR. Elastic-plastic column stability and the design of no-sway frames. Proc. Institution of Civil Engineers 1966; 34:129-152.
- [6] Gent AR, Milner HR. The ultimate load capacity of elastically restrained H-columns under biaxial bending. Proc. Institution of Civil Engineers 1968; 43:685-704.
- [7] Davison JB, Kirby PA, Nethercot DA. Column Behaviour in PR Construction - Experimental Behaviour. ASCE J Struct Eng 1987; 13(9):2032-2050
- [8] Davison JB. Strength of beam-columns in flexibly connected steel frames. Ph.D Thesis. University of Sheffield; 1987
- [9] Gibbons C, Nethercot DA, Kirby PA, Wang YC. An appraisal of partially restrained columns behaviour in non-sway steel frames. Proc. Institution of Civil Engineers, Structures and Buildings 1993; 99:15-28
- [10] Gibbons C, Kirby PA, Nethercot, DA. Experimental behaviour of partially restrained steel columns. Proc. Institution of Civil Engineers, Structures and Buildings 1993;99:29-42
- [11] Gibbons C. The strength of biaxially loaded beam-columns in flexibly connected steel frames. Ph.D. Thesis. University of Sheffield; 1990
- [12] Carr JF. A simplified approach to the design of semi-rigidly connected columns in multi-storey non-sway steel framed buildings. M. Phil Thesis. University of Sheffield;1993
- [13] King, CM Column Design for Axial Compression and End Rotation, PhD Thesis, University of Sheffield, June 2010
- [14] EN 1993-1-1:2005. Eurocode 3: design of steel structures - Part 1.1: General rules and rules for buildings. CEN (European Committee for Standardization); 2005
- [13] EN 10210-2:2006 Hot finished structural hollow sections of non-alloy fine grain steels. Part 2: Tolerances, dimensions and sectional properties. CEN (European Committee for Standardization); 2006
- [16] AISC. Specification for Structural Steel Buildings. ANSI/ AISC 360-10. American Institute of Steel Construction; 2010

Table

Table 1 Test programme		
Test no.	Specimen	Comment
kc1	120 SHS × 5mm	pilot test
kc2	120 SHS × 5mm	pilot test continuation
kc3	120 SHS × 10mm	stable wall thickness
kc4	120 SHS × 10mm	stable wall thickness
kc5	120 SHS × 6.3mm	possible sensitivity to wall slenderness
kc6	120 SHS × 5mm wall	expect sensitivity to wall slenderness
kc7	120 SHS × 10mm wall	stable wall thickness
kc8	120 SHS × 10mm wall	stable wall thickness
kc9	120 SHS × 6.3mm wall	possible sensitivity to wall slenderness
kc10	120 SHS × 5mm wall	expect sensitivity to wall slenderness

Table 2 Material properties				
Specimen	Thickness (mm)	Yield (N/mm ²)	UTS (N/mm ²)	Elongation %
kc1/2	5	396	548	27.5
kc3	10	375	530	35.0
kc4	10	390	530	35.0
kc5	6.3	428	561	25.0
kc6	5	389	540	24.0
kc7	10	not available	not available	not available
kc8	10	375	514	36.5
kc9	6.3	431	549	32.0
kc10	5	402	533	32.0

Table 3 Duration of tests and peak recorded loads				
Test	Time to reach maximum load (mins)	Time from maximum load to end (mins)	Total time (mins)	Maximum Test Load (kN)
kc3	9.4	3.3	12.7	1328
kc4	13.8	5.0	18.8	1458
kc5	10.5	4.3	14.8	915
kc6	10.5	3.6	14.1	695
kc7	11.7	14.7	26.4	1290
kc8	9.9	7.4	17.3	1298
kc9	10.2	6.7	16.9	971
kc10	7.7	2.4	10.1	777

Table 4 End rotation achieved before the onset of local inelastic buckling			
Test columns in single curvature: Column length/external breadth, $L/B = 22$ b/t = internal flat width between radii/thickness			
Test	b/t	Rotation achieved before local inelastic buckling	Comment
kc6, kc10	20	0.040 radians	start of severe local buckling
kc5, kc9	15	0.070 radians	start of loss of stiffness just noticeable
kc3, kc4, kc7, kc8	8	0.095 radians	no sign of loss of resistance before end of test

Table 5 Proposed b/t limits for increasing end rotations	
b/t	Limiting end rotation
26.0	10 (8)
20.2	20 (16)
15.5	36
12.0	58
9.7	83

Figure

[Click here to download Figure: Figure listing.doc](#)

Figure 1 Typical column-beam connection in discontinuous construction

Figure 2 Gent & Milner (a) Experimental arrangement (b) Moment shedding from increasing axial load

Figure 3 Test rig with column in position

Figure 4 Shoe at bottom of test column, in-plane inclinometer and LVDT

Figure 5 Spring grip frame for LVDT connections

Figure 6 Load v mid-height displacement (in-plane)

Figure 7 Out-of-plane mid-height displacement v In-plane mid-height displacement

Figure 8 Axial load v mean end rotation

Figure 9 Normalised axial load v mean end-rotation

Figure 10 Comparison of experimental and simplified rigid-plastic design method axial load v mean end rotation

Figure 11 Axial load v mean end rotation for 5mm and 6.3 mm wall thicknesses

Figure 12 Abaqus FE model (shell elements)

Figure 13 Assumed residual stress pattern (same on all four faces)

Figure 14 Effect of in-plane end rotation on axial load resistance for a range of wall thicknesses

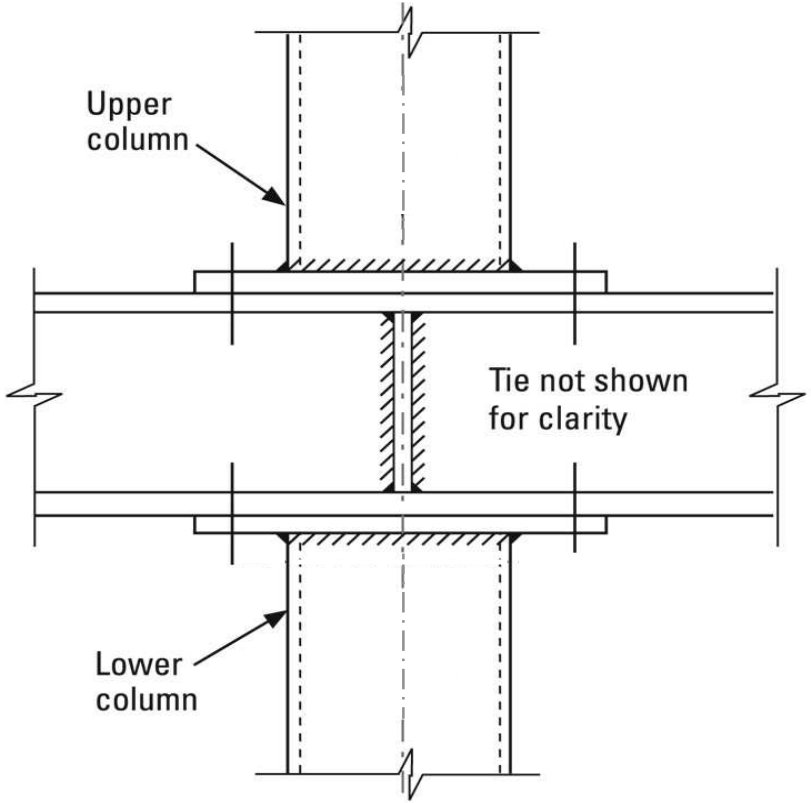
Figure 15 Effect of end rotation on a 45° plane on axial resistance for a range of wall thicknesses

Figure 16 Design limits for 140x140SHS in 355MPa steel in single curvature

Figure 17 Comparison of experimental and FEA axial compression v end rotation for (a) Test kc6 (b) Test kc10

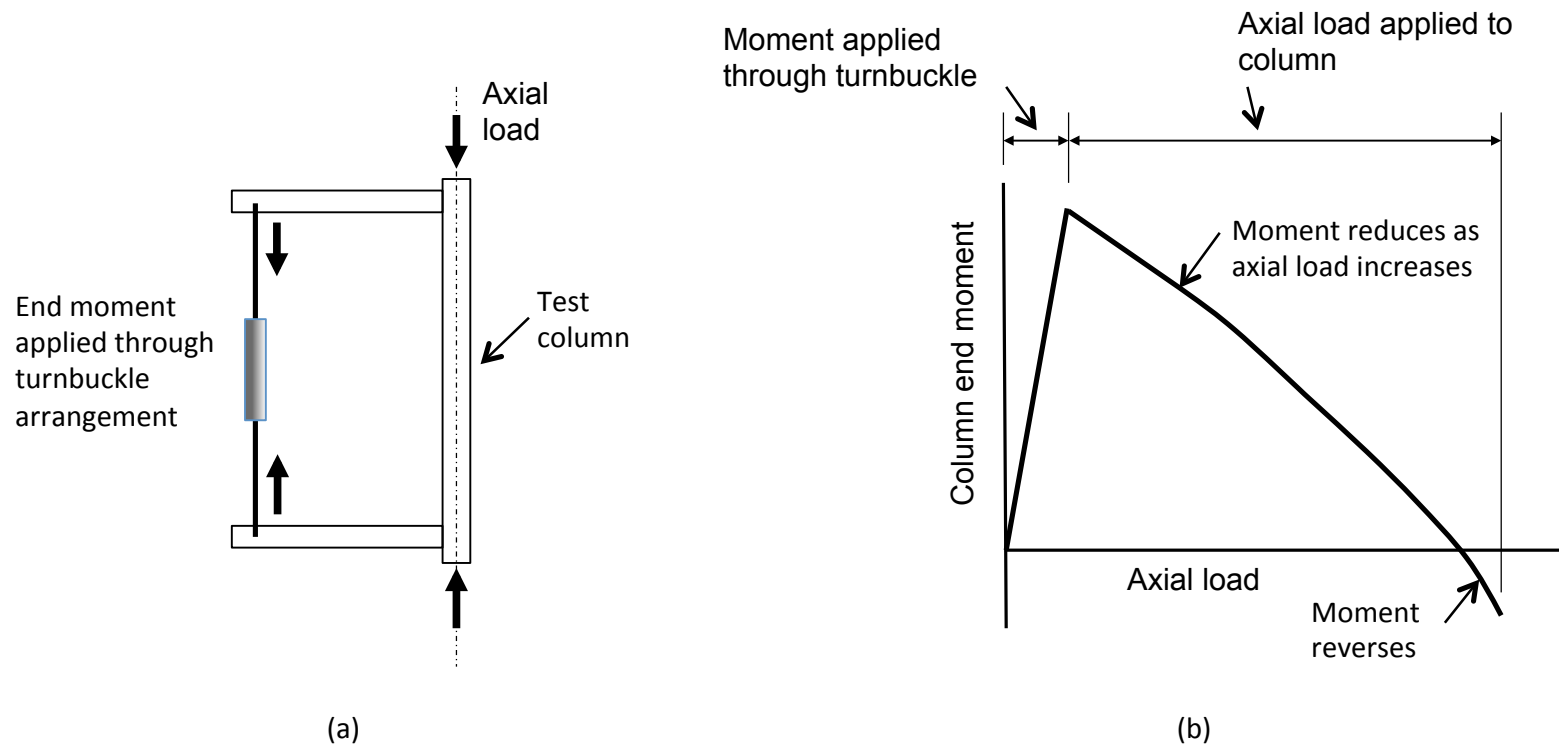
Figure

[Click here to download Figure: Figure 1.pdf](#)



Figure

[Click here to download Figure: Figure 2.pdf](#)



Figure

[Click here to download Figure: Figure 3.pdf](#)



Figure

[Click here to download Figure: Figure 4.pdf](#)



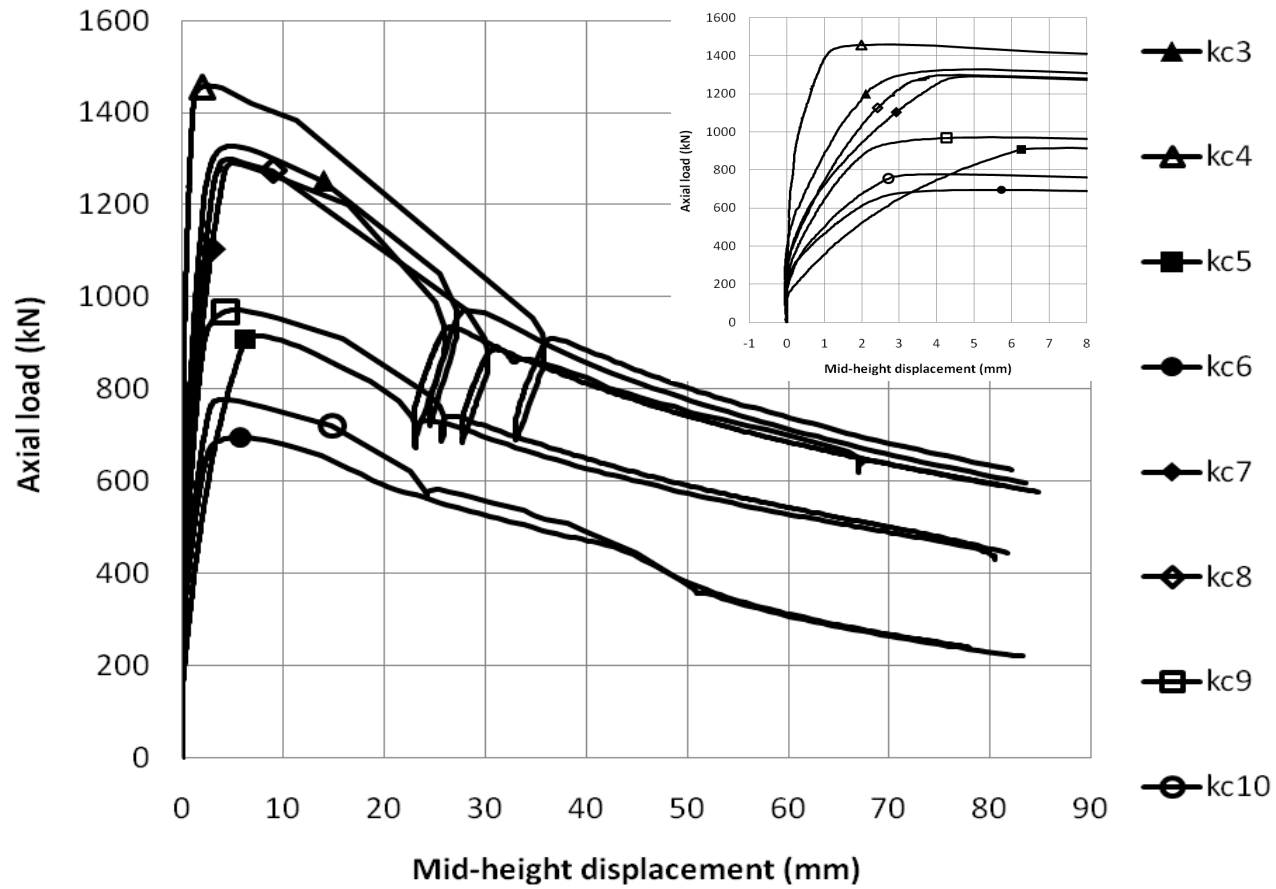
Figure

[Click here to download Figure: Figure 5.pdf](#)



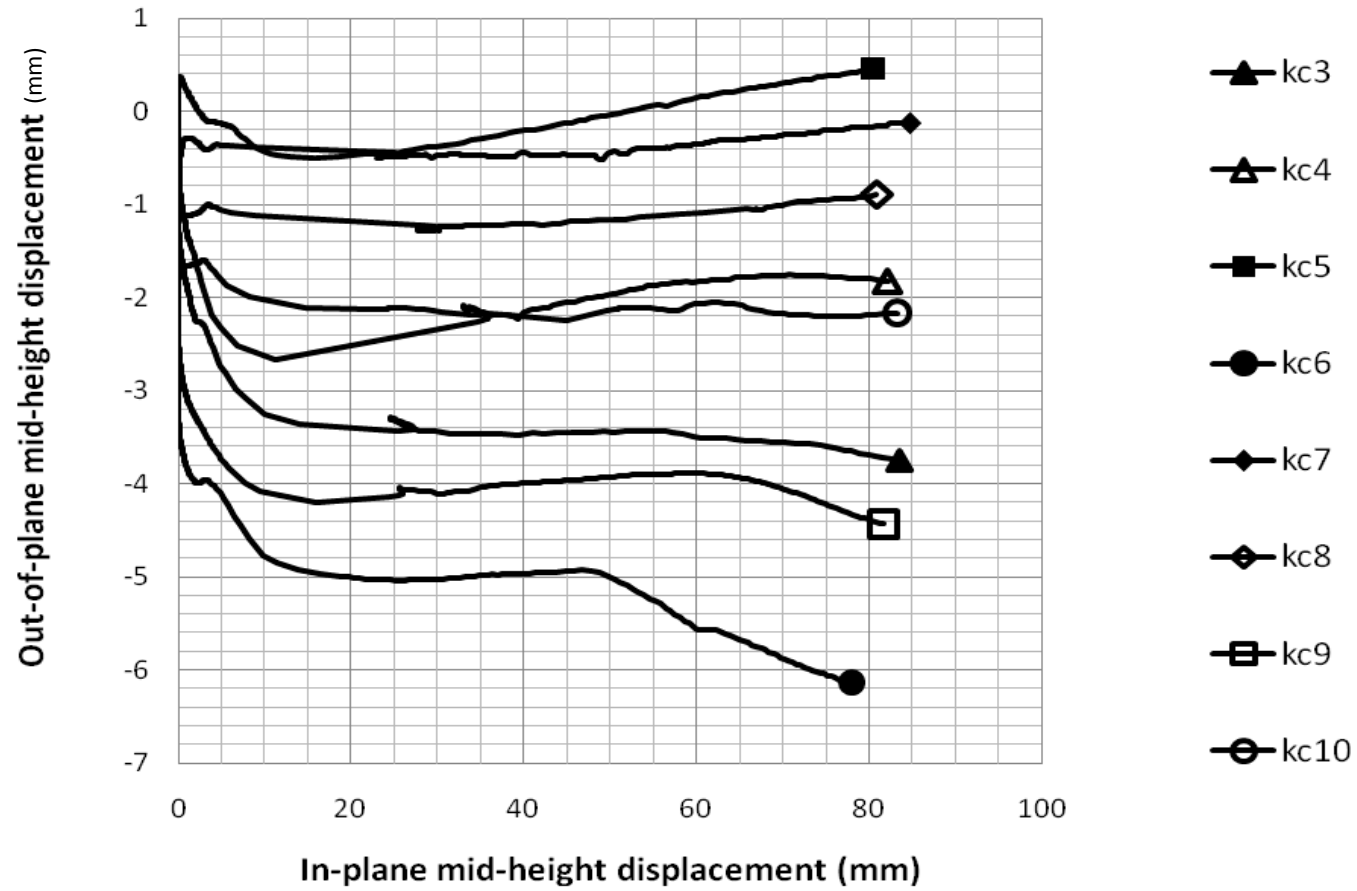
Figure

[Click here to download Figure: Figure 6.pdf](#)



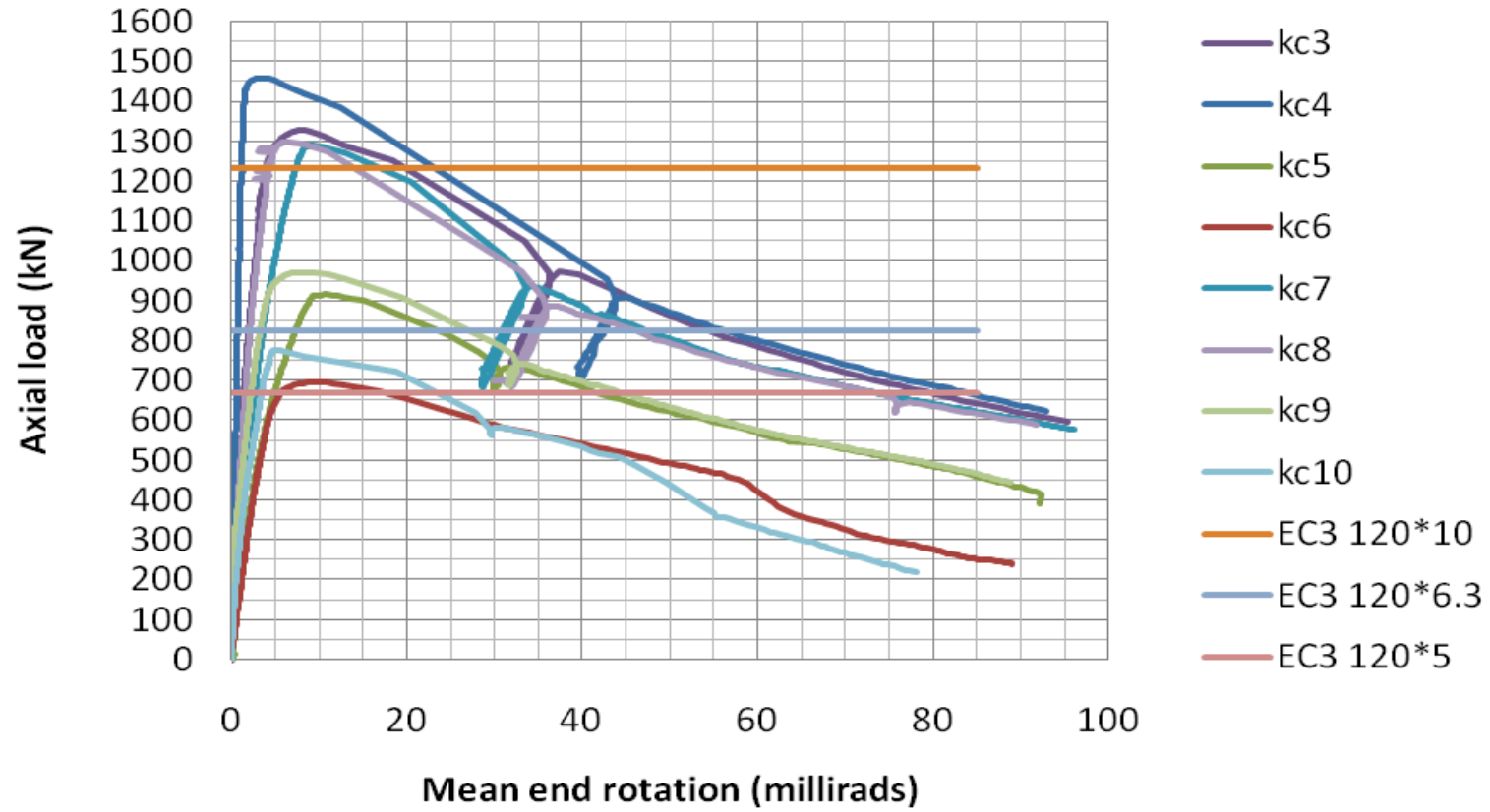
Figure

[Click here to download Figure: Figure 7.pdf](#)



Figure

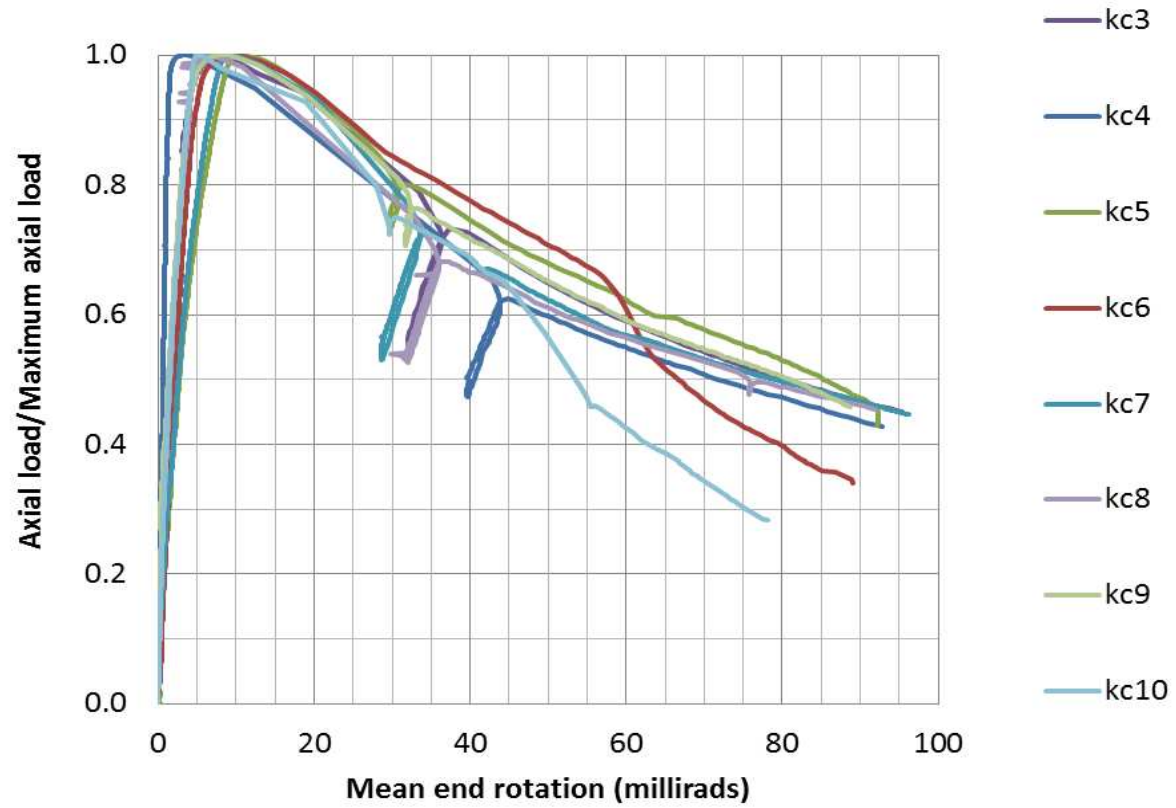
[Click here to download Figure: Figure 8.pdf](#)



Figure

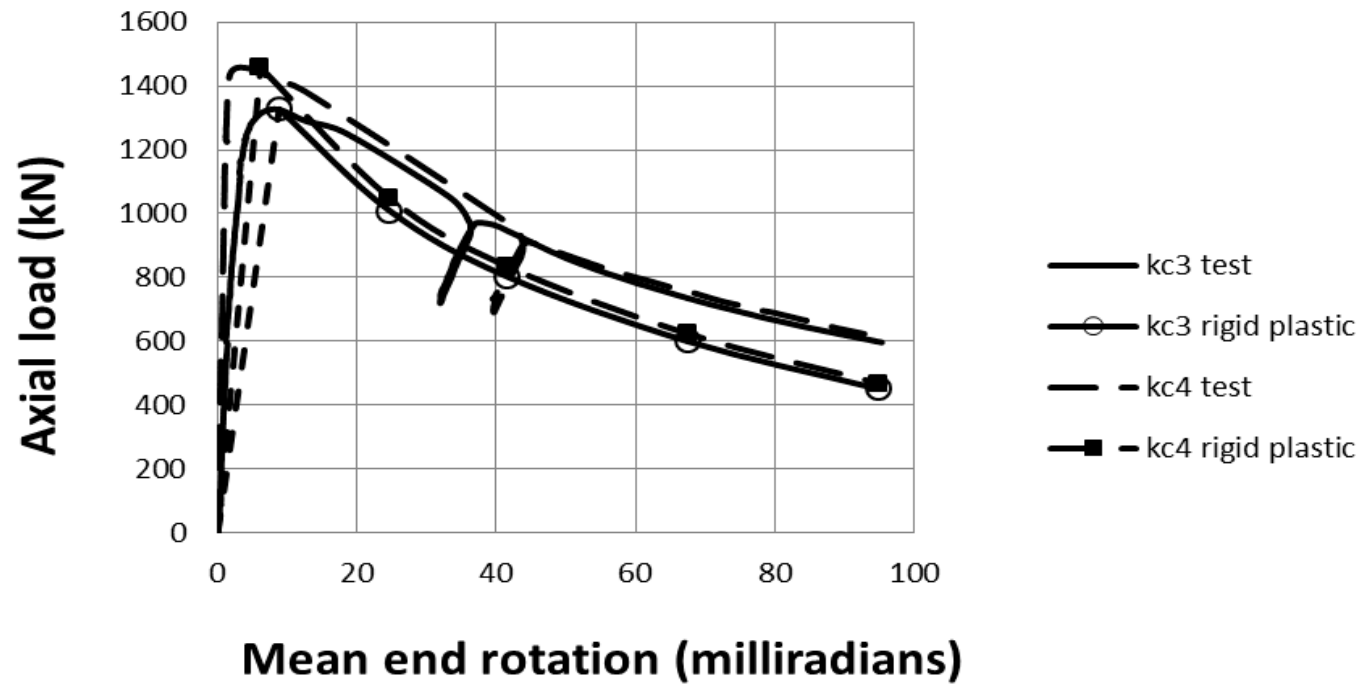
[Click here to download Figure: Figure 9.pdf](#)

kc3 to kc10; normalised axial v mean end rotation



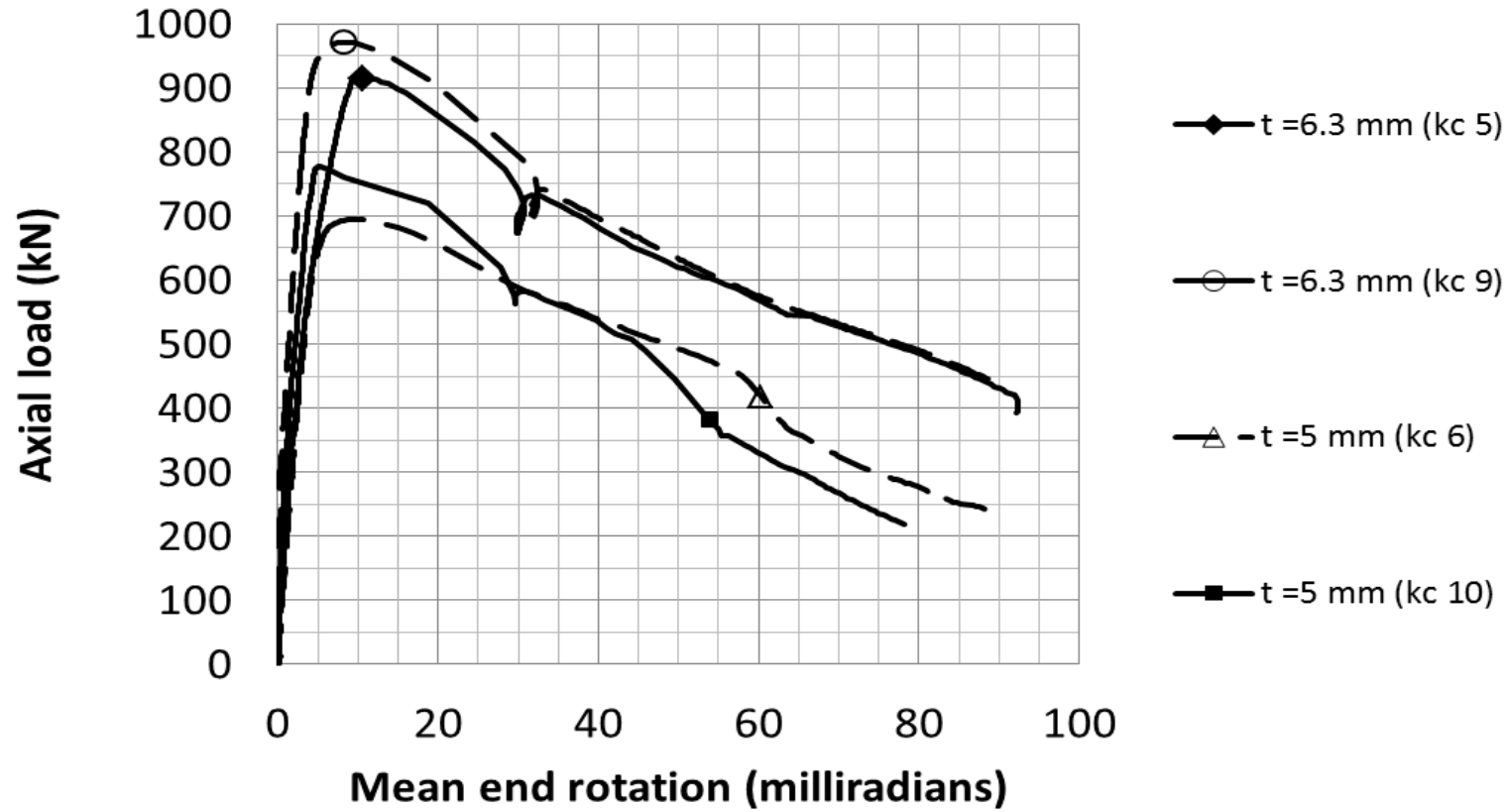
Figure

[Click here to download Figure: Figure 10.pdf](#)



Figure

[Click here to download Figure: Figure 11.pdf](#)



Figure

[Click here to download Figure: Figure 12.pdf](#)

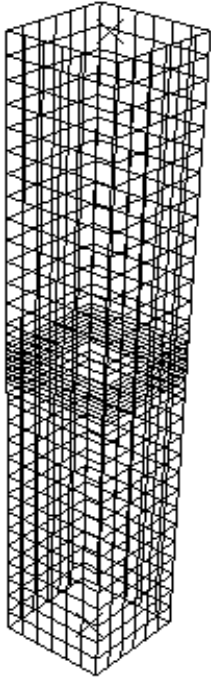
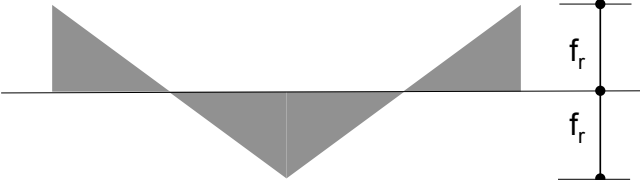
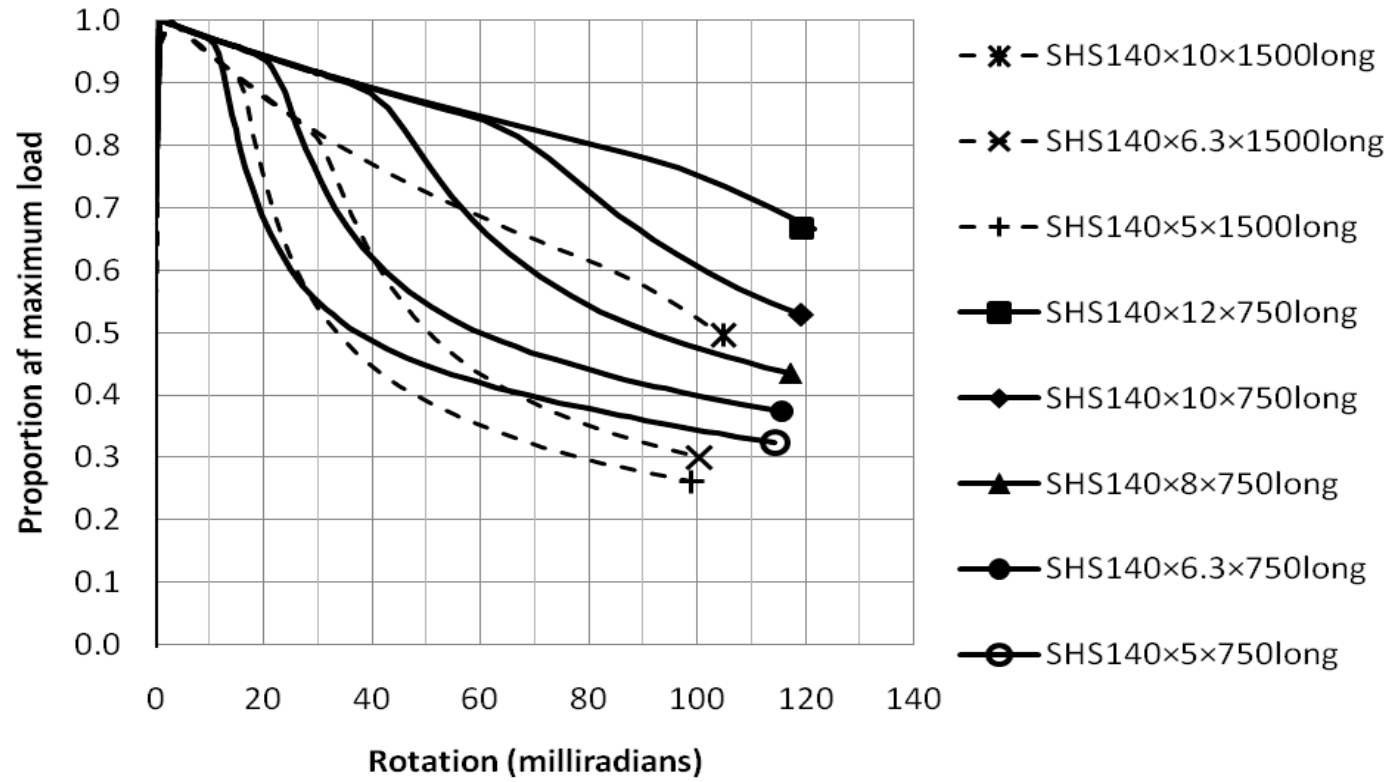


Figure
[Click here to download Figure: Figure 13.pdf](#)



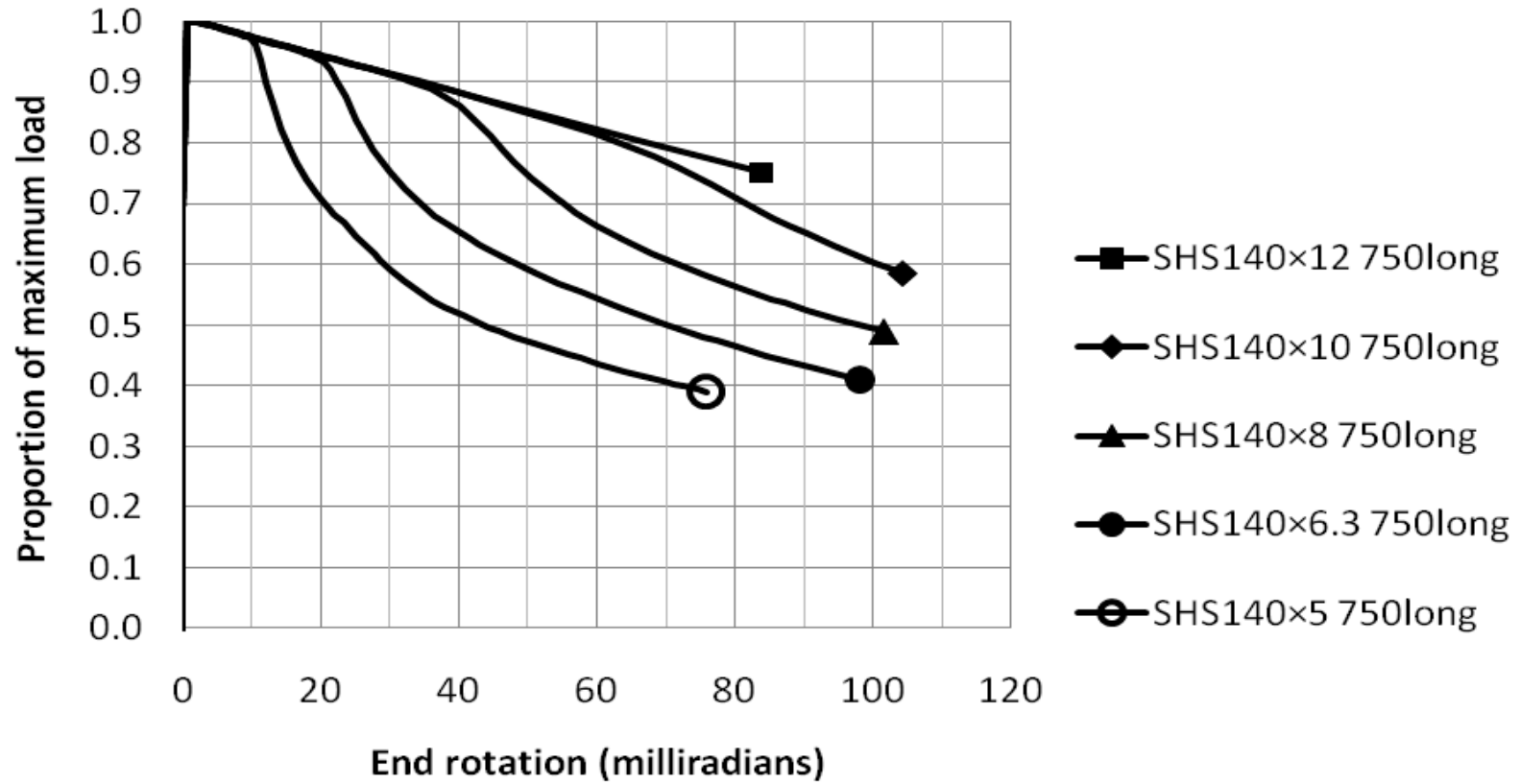
Figure

[Click here to download Figure: Figure 14.pdf](#)



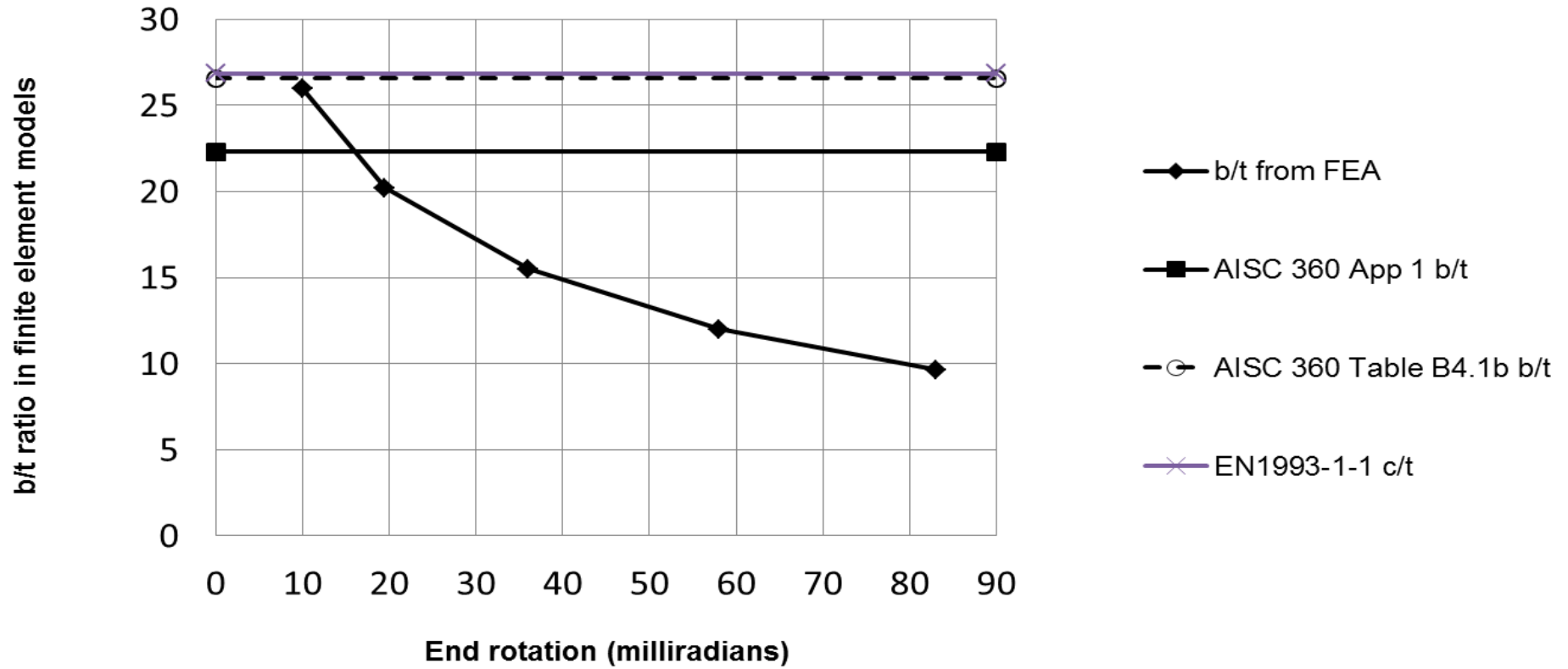
Figure

[Click here to download Figure: Figure 15.pdf](#)



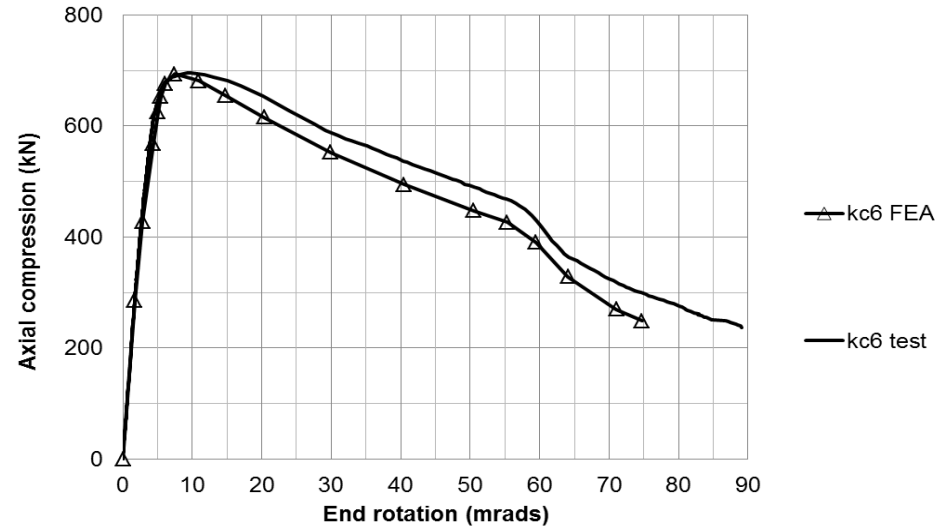
Figure

[Click here to download Figure: Figure 16.pdf](#)

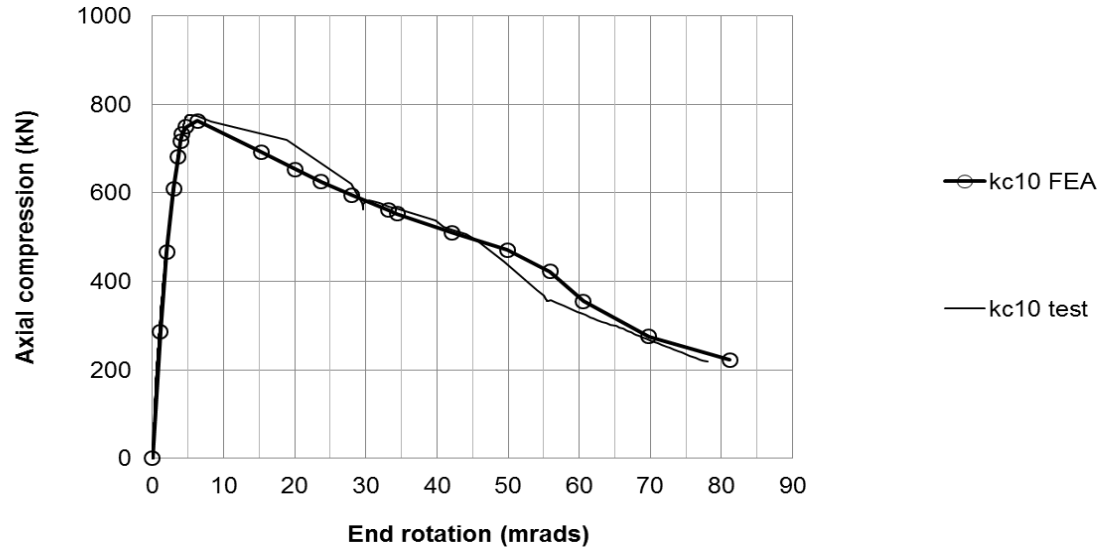


Figure

[Click here to download Figure: Figure 17.pdf](#)



(a)



(b)